JOURNAL OF APPLIED ELECTROCHEMISTRY **27** (1997) 1045–1051

Influence of solid phase conductivity on spatial localization of electrochemical processes in flow-through porous electrodes

Part II: Nonuniform porous matrix with a variable conductivity profile

A. I. MASLIY, N. P. PODDUBNY

Institute of Solid State Chemistry, Siberian Branch of Russian Academy of Sciences, Novosibirsk, Russia

Received 27 March 1996; revised 10 December 1996

The possibilities of improving the current distribution uniformity of the main reaction and of increasing porous electrode (PE) performance efficiency by using a porous matrix with a definite profile of conductivity $\kappa_s(x)$ have been theoretically analysed. A more general deduction of an equation for the $\kappa_s(x)$ profile providing the electrode with constant polarization is given. Peculiarities of this profile and ways of its approximate realization are discussed. The possibility of significant increase in the performance efficiency of electrodes of this type has been experimentally confirmed.

Keywords: *Solid phase conductivity, Flow-through porous electrodes, Performance efficiency, Conductivity, Polarization*

Nomenclature

$P(x), \phi(x)$	local potentials in the solid and liquid phases (V)
$\eta(x)$	polarization (V)
i	local current density ($\mathrm{A\,cm^{-2}}$)
i_a, i_g	modulus of average and total (geometric) current densities ($\mathrm{A\,cm^{-2}}$)
i_{max}, i_{min}	maximum and minimum current densities ($\mathrm{A\,cm^{-2}}$)
κ_s, κ_L	solid and liquid phase conductivities ($\Omega^{-1}\mathrm{cm^{-1}}$)
κ_i	conductivity of the solid phase of ith layer of the multilayer PE ($\Omega^{-1}\mathrm{cm^{-1}}$)
S_v	specific surface of PE ($\mathrm{cm^{-1}}$)
S_{eff}	effective working surface of PE ($\mathrm{cm^2}$)
u	linear rate of the solution flow ($\mathrm{cm\,s^{-1}}$)
L	overall thickness of PE (cm)
L_i	thickness of the ith layer of the multilayer PE (cm)
L_{eff}	effective working thickness of PE taking account of the zones of current density lower than limiting (cm)
k_0, k_L, k	truncation coefficients of the edges of hyperbolic profiles of solid-phase conductivity
γ	factor of proportionality between current density and polarization for the linear polarization curve ($\Omega^{-1}\mathrm{cm^{-2}}$)
V	solution volume ($\mathrm{cm^3}$)
c_0, c_t	initial and final electroactive component concentrations ($\mathrm{mol\,cm^{-3}}$)
k_m	mass transfer coefficient ($\mathrm{cm\,s^{-1}}$)

1. Introduction

Geometrically unequal accessibility of different points on the surface of a porous electrode (PE) with a uniformly conducting matrix inevitably leads to electrical nonuniformity, nonuniform potential and current distribution over the PE depth. In this case smoothing of the current distribution is attained only due to electrochemical factors, such as polarization resistance at the electrode-solution interface. As shown earlier [1], these possibilities are the wider the less is the height and the greater is the width of the limiting current plateau of the main electrochemical reaction. If the main reaction proceeds over a narrow range of potentials or at a moderate or high electroactive component concentration, the smoothing possibilities of electrochemical factors turn out to be limited and the working thickness of the PE turns out to be small.

In this case, the increase in the effective working thickness of a PE can be obtained only due to additional factors. It is evident from the analysis of current passage through the auxiliary and the working electrodes that these factors may be associated only with the regions where the current passes over the solid or liquid phase (exactly, with the conductivities of these regions). Since it is difficult to create a stable conductivity profile in the liquid phase, the only real factor to be affected is the conductivity of the solid phase. The idea of using the solid phase conductivity (or additional resistances connected to the different-distant regions of the working electrode) in order to influence the potential and current distribution is not

0021-891X

new. Additional resistances have been connected to elements of a segmented electrode in order to attain their equipotentiality [2, 3]. This idea has been of interest up to now [4–6].

Application of the solid phase conductivity for compensation of geometrically unequal accessibility of different points of a PE was first suggested in an earlier paper [7]. A peculiarity of our approach was a special attention to the locally changing solid phase conductivity and the search for a $\kappa_s(x)$ profile such as to ensure attainment of an ideally uniform current and potential distribution. The validity of the obtained $\kappa_s(x)$ profile was later confirmed [8]. Although the method suggested for the regulation of PE work is not universal and cannot be used, for example, in metal deposition processes, it is promising for a rather wide range of redox reactions where the specially created $\kappa_s(x)$ profile does not change during the reaction. Thus, in this paper we return to the idea of optimization of a PE by nonuniform resistance of the porous matrix in order to analyse its possibilities and to explore the realization of this idea and correlation with experiment.

2. Mathematical formulation of the problem

To facilitate comparison with the previous results [9], we use the same physical model and modified mathematical model of a PE. Taking into account variable conductivities of the solid and liquid phases, the boundary problem for the distribution of potentials over a PE can be described by the following system of equations:

$$\frac{\mathrm{d}}{\mathrm{d}x}\left(\kappa_s(x)\frac{\mathrm{d}P}{\mathrm{d}x}\right) = S_v i(\eta) \tag{1}$$

$$\frac{\mathrm{d}}{\mathrm{d}x}\left(\kappa_L(x)\frac{\mathrm{d}\phi}{\mathrm{d}x}\right) = -S_v i(\eta) \tag{2}$$

with the boundary conditions:

$$\left.\frac{\mathrm{d}P}{\mathrm{d}x}\right|_{x=L} = \left.\frac{\mathrm{d}\phi}{\mathrm{d}x}\right|_{x=0} = 0 \tag{3}$$

$$\left.\frac{\mathrm{d}P}{\mathrm{d}x}\right|_{x=0} = \frac{i_g}{\kappa_s(0)} \tag{4}$$

$$\left.\frac{\mathrm{d}\phi}{\mathrm{d}x}\right|_{x=0} = \frac{i_g}{\kappa_L(0)} \tag{5}$$

Here

$$\eta(x) = P(x) - \phi(x) \tag{6}$$

and $i(\eta)$ is the overall polarization curve involving the main and side reactions. Preliminary attempts to solve the border problem described above according to the target method on the basis of Runge–Kutt procedures [10] have shown that the presence of the derivatives $\mathrm{d}\kappa_s(x)/\mathrm{d}x$ and $\mathrm{d}\kappa_L(x)/\mathrm{d}x$ in Equations 1 and 2 and the elevated sensitivity of the method to local gradients of phase conductivities often lead to very slow convergence or even to instability of the solution. Therefore, to obtain stable results of calculations, the boundary problem should be modified (Equations 1–5). For this purpose, Equations 1 and 2 are integrated from 0 to x. Then, taking into account the boundary condition (Equation 3) we obtain

$$\kappa_s(x)\frac{\mathrm{d}P}{\mathrm{d}x} - i_g = S_v I(x) \tag{7}$$

$$\kappa_L(x)\frac{\mathrm{d}\phi}{\mathrm{d}x} = -S_v I(x) \tag{8}$$

where $I(x) = \int_0^x i(\eta(\tau)\mathrm{d}\tau)$ is the total current passing through the part of a PE from the back current-feeder to the section x.

Having divided Equation 7 by $\kappa_s(x)$ and Equation 8 by $\kappa_L(x)$ and subtracted the latter from the former, we obtain

$$\frac{\mathrm{d}\eta}{\mathrm{d}x} - \frac{i_g}{\kappa_s(x)} = \left(\frac{i_g}{\kappa_s(x)} + \frac{i_g}{\kappa_L(x)}\right) S_v I(x) \tag{9}$$

As a result, solving the boundary problem is transformed into solving Equation 9, the integro-differential equation, with the following additional condition:

$$\left.\frac{\mathrm{d}\eta}{\mathrm{d}x}\right|_{x=L} = \frac{i_g}{\kappa_L(L)} \tag{10}$$

The equations for the concentration field in a PE and for the overall polarization curve including the main and side-electrochemical processes, as well as the values of kinetic parameters, remain the same as in [9]. The change in equilibrium potential of the main process over the electrode depth was not taken into account.

Since $\kappa_s(x)$ and $\kappa_L(x)$ in Equation 9 lie outside the differentiation, this equation does not require that the derivatives of the phase conductivity profiles should be continuous. This allows solution of problems involving stepwise profiles. To solve Equation 9 numerically, we used the target method from one end of the PE to the other. To do this $\eta(x)$ is expressed in terms of $\mathrm{d}\eta/\mathrm{d}x$:

$$\eta(x) = \eta(0) + \int_0^x \frac{\mathrm{d}\eta}{\mathrm{d}x}(\tau)\mathrm{d}\tau \tag{11}$$

Application of the trapezoid rule to the integrals in Equations 9 and 11 and the Euler method to the discharging ions transfer equation (see Equation 2 in [9]), at any x, results in a nonlinear equation for $\mathrm{d}\eta/\mathrm{d}x$ which can be solved, for example, by the Newton method. The value $\eta(0)$ is calculated by the bisection method to satisfy the boundary condition (Equation 10). The current balance condition was also fulfilled, as well as the stability of the solution for duplicated number of subdivision points over the PE depth.

3. Results and discussion

3.1. *Porous electrode with constant* η

Let us consider an ideal case with complete compensation of the geometrically unequal accessibility of different points of a PE due to local changes in $\kappa_{\mathrm{s}}(x)$. As mentioned above, this problem was first set up and solved in [7]. In this paper we suggest a new (more simple and general) derivation of $\kappa_{\mathrm{s}}(x)$ for a PE with constant (equal) polarization. From the condition $\eta = \mathrm{const}$, it follows that, at any point, $\mathrm{d}\eta/\mathrm{d}x = 0$ and $i(\eta) = -i_{\mathrm{a}}$. The last equation, in the strict sense, is valid provided that the current density is dependent only on the polarization and is not a function of the point. In this case, the polarization curve $i(\eta)$ throughout the PE is the same, and the shape of this dependence is insignificant.

Substituting the values of $\mathrm{d}\eta/\mathrm{d}x$ and $i(\eta)$ into the integro-differential equation (Equation 9) and taking into account that $I(x) = -i_{\mathrm{a}}x$ and $i_{\mathrm{g}} = S_{\mathrm{v}}Li_{\mathrm{a}}$, we have

$$\frac{L}{\kappa_{\mathrm{s}}(x)} = \left(\frac{1}{\kappa_{\mathrm{s}}(x)} + \frac{1}{\kappa_{\mathrm{L}}(x)}\right)x \qquad (12)$$

from which, after some transformations for $\kappa_{\mathrm{L}} = \mathrm{const}$, we obtain

$$\kappa_{\mathrm{s}}(x) = x_{\mathrm{L}}\left(\frac{L}{x} - 1\right) \qquad (13)$$

It is evident that for the attainment of an ideally uniform current and potential distribution with the polarization curve of arbitrary shape it is necessary that:

(i) Conductivity of the solid porous matrix should be decreased over the depth of the PE from infinity at the point near the back current-feeder ($x = 0$) to 0 at the front end of the electrode ($x = L$).
(ii) At the middle point of the electrode, effective conductivities of the solid and liquid phases should be equal.

3.2. *Influence of limitations of the maximum and minimum values of hyperbolic profile $\kappa_{\mathrm{s}}(x)$ on the nonuniformity of the current distribution within PE*

Attempts to realize the hyperbolic conductivity profile of this type (Equation 13) encounter difficulties associated primarily with its ends, because the infinite and zero conductivities of porous matrices are the most difficult for realization. Real porous electrode materials (e.g., fibrous carbon [11]) have finite values of conductivity. From this point of view, it is important to evaluate the influence of limitations at the ends of the profile on the nonuniformity of current distribution over the electrode depth. We used the following limitations for $\kappa_{\mathrm{s}}(x)$: solid phase conductivities tending to zero (at the front end) and to infinity (at the current-feeder) were replaced by more natural finite values $\kappa_{\mathrm{s}}(0) = k_0\kappa_{\mathrm{L}}$ and $\kappa_{\mathrm{s}}(L) = \kappa_{\mathrm{L}}/k_{\mathrm{L}}$, where k_0 and k_{L} are truncation coefficients. In symmetric cutting, $k_0 = k_{\mathrm{L}} = k$. For simplicity, the influence of cutting can be illustrated with the case of the linear polarization curve $i = \gamma\eta$ as an example.

An unlimited hyperbolic profile $\kappa_{\mathrm{s}}(x)$ and a profile with the above-mentioned symmetrical limitations at the ends are shown in Fig. 1 (curves (a) and (a′)). Current distributions corresponding to these profiles are also shown. The hyperbolic profile without limitations gives an ideally uniform current distribution over the entire electrode depth (curve (b)). Introduction of the limitations results in a distribution of current similar to the uniform one only in the electrode region approximately corresponding to the hyperbolic region of the profile. In the regions of limitations at the ends of the electrode the current distribution of parabolic shape with a minimum (curve (b′)), which is typical of regions with constant solid phase conductivity, is observed. It can be seen from Fig.1 that even with the symmetrical cutting of the profile $\kappa_{\mathrm{s}}(x)$ and approximately the same spatial localization of the nonuniform current distribution at both ends of the electrode, the negative effect of limitations at the front end is much greater than at the back end.

As opposed to the ideally hyperbolic profile (Equation 13), which is not sensitive to the shape of the polarization curve (in particular, to its slope), deterioration of the current distribution with limitations at a fixed value of k is essentially dependent on the slope of the polarization curve. A practically nonpolarizable electrode is the most sensitive to the limitations at the ends of the $\kappa_{\mathrm{s}}(x)$ profile. On the contrary, for systems with high polarizability, limitations of the profile (Equation 13) have only a slight impact on the current distribution up to the very low values of the threshold of cutting. Numerical calculations show that the limitation of the profile provides local influence only at that end of the electrode where it was introduced. No marked cross effect of limitations was observed.

Thus, the replacement of the infinite and zero conductivity at the ends of the hyperbolic profile $\kappa_{\mathrm{s}}(x)$ by finite values results in local distortions in the uniform current distribution in the region with the introduced limitations, which are the greater the

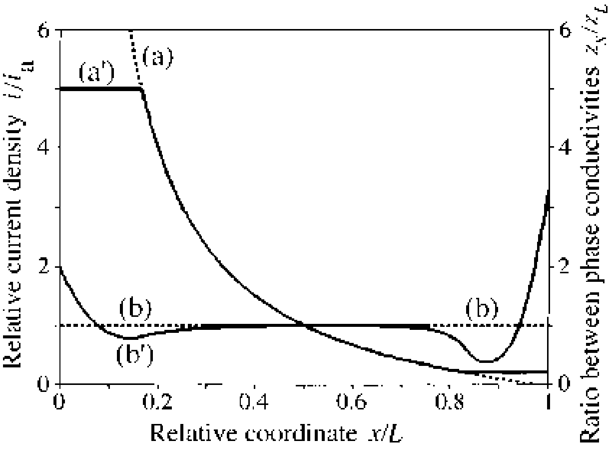

Fig. 1. Hyperbolic profile of the changes in the solid phase conductivity without limitations (a) and with symmetric limitations at the ends of the electrode (a′) and corresponding profiles of the current distribution (b, b′). $\kappa_{\mathrm{L}} = 0.1\,\Omega^{-1}\,\mathrm{cm}^{-1}$, $S_{\mathrm{v}} = 125\,\mathrm{cm}^{-1}$, $L = 0.2$ cm, $k = 5$, $\gamma = 0.8\,\Omega^{-1}\,\mathrm{cm}^{-2}$.

lower is the threshold of cutting and the electrode polarizability. To smooth over the distortions, it is necessary to attain minimum possible thickness of layers with constant solid phase conductivity, especially at the front end of the electrode.

3.3. *Approximate realization of the hyperbolic profile of* $\kappa_s(x)$

Unfortunately, difficulties arising in the realization of the ideal profile $\kappa_s(x)$ are not reduced to the limitations at the ends of the electrode. Another problem is the absence of the porous electrode materials with a continuous profile of conductivity (including ones of required hyperbolic type). At the same time, industry produces sheet fibrous carbon materials with different conductivities [12, 13]. Therefore, it is possible to obtain the necessary profile of conductivity by combining layers of different electrode materials. Naturally, the greater the number of layers and the thinner they are, the more exactly hyperbolic is the profile shape and the more uniform is the current distribution over the electrode depth. However, the number of materials similar in type and different in conductivity is not so large. Hence, it is important to evaluate the scale of possible improvement of the current distribution uniformity for limited numbers of layers and to find the optimal way of searching for the required thickness and conductivity of the layer. As in the previous section, the numerical simulation of the PE work was based on the simplest (linear) shape of the polarization curve.

Figure 2 presents profiles of the solid phase conductivity (curves (a)–(c)) and Fig.3 shows the corresponding curves of the relative current density over the electrode depth ((a′)–(c′)) for different numbers of layers of porous material. An electrode composed of only one layer was chosen as an initial case. For electrode thickness of 0.2 cm, solid and liquid phase conductivities of 0.1 Ω^{-1} cm^{-1} and $\gamma = 0.8\,\Omega^{-1}$ cm^{-2}, the observed current distribution is symmetric about the electrode centre (curve (a′)) but is, nevertheless, remarkable for its high nonuniformity (a ratio $i_{\max}/i_{\min} = 44.1$).

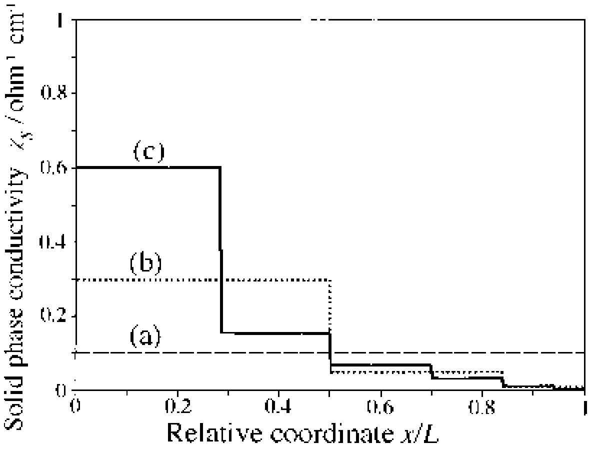

Fig. 2. Profiles of solid phase conductivity ((a)–(c)). See also Fig. 3.

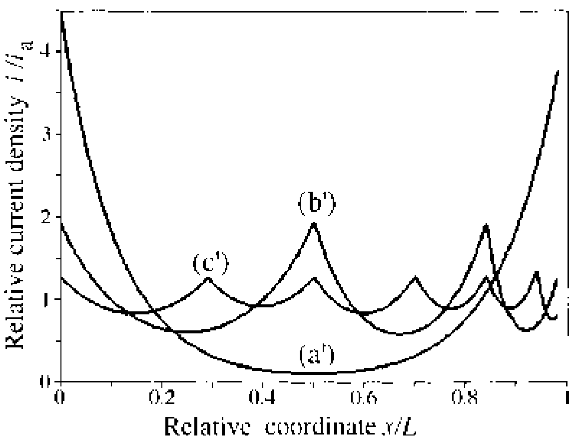

Fig. 3. Associated distributions of relative current density along the depth of PE ((a′)–(c′)) for different number of layers: (a), (a′) 1; (b), (b′) 3; (c), (c′) 6. Other parameters are the same as in Fig. 1.

Next we consider a porous electrode with the same thickness composed of three layers of electrode materials with the following conductivities κ_i (Ω^{-1} cm^{-1}) and thicknesses of the layers obtained by optimization of L_i (cm): $\kappa_1 = 0.3$, $L_1 = 0.1$; $\kappa_2 = 0.049$, $L_2 = 0.068$; $\kappa_3 = 0.0087$, $L_3 = 0.032$. The optimum condition involves attainment of the maximum uniformity of the current distribution on each layer of the electrode material. As a first approximation, the thickness of the layers were taken to be equal and conductivities of the layers related to their middle points were calculated from Equation 13. The coordinates of boundaries of the layers were then changed in such a way as to attain smoothing of the current distribution over all the layers. In this case, the hyperbolic law for $\kappa_s(x)$, related to the middle points of the layers, was valid. The optimal profile of $\kappa_s(x)$ and the corresponding current distribution obtained in the process are represented by the curves (b) and (b′). It is evident that the general pattern of the current distribution includes three regions with a symmetrical parabolic distribution in each layer. With the optimal choice of κ_i and L_i, the ratio $i_{\max}/i_{\min}$ is the same in each layer and is equal to 3.24.

Analogous simulation of the electrode consisting of six layers of porous materials was conducted at the same L and the following values of κ_i and L_i: $\kappa_1 = 0.6$, $L_1 = 0.057$; $\kappa_2 = 0.155$, $L_2 = 0.043$; $\kappa_3 = 0.67$, $L_3 = 0.04$; $\kappa_4 = 0.3$, $L_4 = 0.028$; $\kappa_5 = 0.0124$, $L_5 = 0.02$; $\kappa_6 = 0.0027$, $L_6 = 0.012$. The profile of conductivity and the current distribution for this case are represented by curves (c) and (c′). It is apparent that a twofold increase in the number of layers results in practically proportional improvement of the current distribution $i_{\max}/i_{\min} = 1.6$.

It should be noted that when the hyperbolic profile $\kappa_s(x)$ is changed by a stepwise profile corresponding to a small number of layers, the sets of layers with unequal thickness turn out to be optimal with respect to the current distribution uniformity. In this case, contrary to what might be expected from Equation 13, the layer possessing the highest conductivity has the largest thickness and the layer with the lowest conductivity has the smallest one. Numerical analysis of the influence of different factors also shows that the relative gain in the current distribution uniformity for a complex porous electrode with variable conductivity of layers in comparison with a one-layer electrode of the same thickness increases with increasing total thickness and decreasing electrode polarizability.

3.4. *Comparison of the efficiency of the PE work with constant and variable solid phase conductivity*

As indicated above, variable solid phase conductivity is very promising for the improvement of PE efficiency for conducting, primarily, redox reactions. Since such reactions have no physical effect on the PE surface, the use of the above direct indicators of the current distribution uniformity for experimental comparison of two types of PE is difficult. It is better to use indirect indicators for this purpose, for example, the part of the surface working at the limiting current (see [14, 15]). Furthermore, the above linear polarization curve is far from being real and does not take into account side reactions. Therefore, in this section we consider theoretically and experimentally the efficiency of three-layer electrodes with constant and variable layers conductivity for a real cathodic process including the main redox reaction and the side process of hydrogen evolution using criteria that can be checked experimentally.

Theoretical evaluation of the efficiency of the internal PE surface was performed analogously to [9]. For this purpose, two different electrodes (with constant solid phase conductivity and one changing stepwise) were taken and the current density distribution was calculated for different current loads. From the analysis of these distributions, the overall thickness of layers working at the limiting diffusion current and the effective working thickness L_{eff} allowing for the total current of the main reaction were determined. Kinetic parameters of the redox reaction and hydrogen evolution were taken to be the same as in [9].

The thickness of a PE with constant conductivity of the porous matrix ($\kappa_s = \kappa_L = 0.1\,\Omega^{-1}\,\mathrm{cm}^{-1}$) and the summary thickness of the layers of the three-layer electrode were equal (0.8 cm). In the latter case it is suggested that different layers of the electrode material differ only by their conductivities. The boundaries of the layers were constant and corresponded (in relative units) to optimal coordinates of boundaries obtained in calculations with linear polarization.

Figure 4 presents profiles of the current density distribution of the main redox reaction for one- and three-layer electrodes at different average current densities. With allowance for the equality of the solid and liquid phase conductivities, the current distribution in a one-layer electrode (curve (a)) is approximately symmetrical and includes two loaded regions (at the ends of the electrode) and the middle part which is practically inoperative. Taking into account that curve (a) illustrates the near-limiting possibility of the main reaction to penetrate inside the one-layer electrode, it is apparent that this possibility is highly restricted. At smaller average current load, the working zone is reduced, and a further increase in the current load leads only to higher hydrogen evolution (Fig. 5, curves (a) and (a′)). Thus, though the profile of the current distribution for the one-layer electrode with equal effective conductivities of the solid and liquid phases considerably differs from the monotonic profile for infinite solid phase conductivity, the dependence of the effective working thickness of the PE on the current density is the same in both cases. When the average current density attains values such that, at the loaded parts of the electrode hydrogen evolution begins, further penetration of the main reaction into the PE is practically stopped.

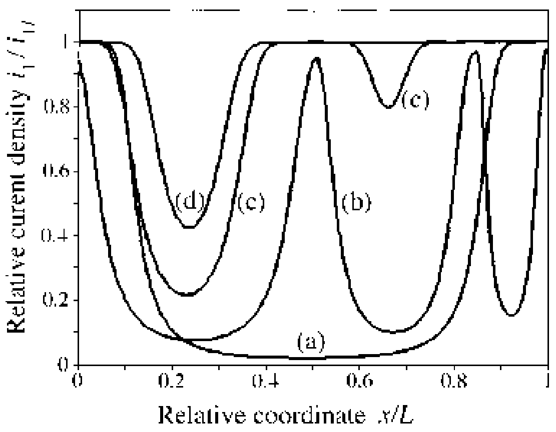

Fig. 4. Profiles of current density distribution of main reaction over the thickness of one-layer (a) and three-layers ((b)–(d)) porous electrodes for different values of the average current density (mA cm^{-2}): (a), (b) 10; (c) 20; (d) 30. Parameters of the electrode: $L = 0.8$ cm, $\kappa_s = \kappa_L = 0.1\,\Omega^{-1}\,\mathrm{cm}^{-1}$ (for one-layer electrode); $\kappa_1 = 0.3\,\Omega^{-1}\,\mathrm{cm}^{-1}$, $L_1 = 0.4$ cm; $\kappa_2 = 0.0492\,\Omega^{-1}\mathrm{cm}^{-1}$, $L_2 = 0.272$ cm; $\kappa_3 = 0.0087\,\Omega^{-1}\,\mathrm{cm}^{-1}$, $L_3 = 0.128$ cm (for three-layer one). Kinetic parameters of the main and side reactions were the same as in [9].

For the three-layer electrode with variable layer conductivity, the profile of the current distribution at low values of the average current density (curve (b),

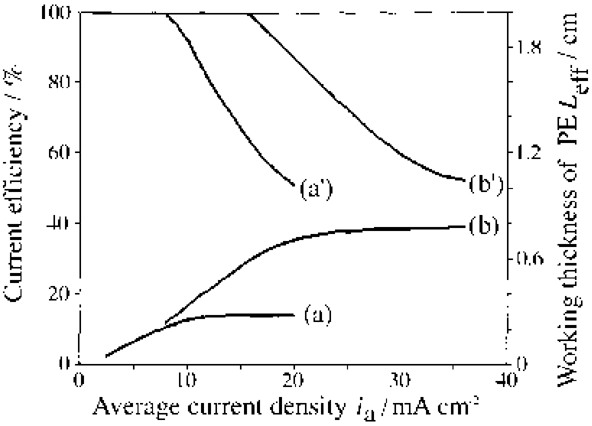

Fig. 5. Influence of average current density on effective working thickness L_{eff} ((a), (b)) and current efficiency ((a′), (b′)) of main reaction for porous electrodes with constant ((a), (a′)) and three-stepwise changing solid phase conductivity ((b), (b′)). Based on data from Fig. 3.

Fig. 3) consists of three parts corresponding to separate porous layers. Due to the existence of loaded zones in each part, the overall efficiency of PE performance increases considerably. With increasing average current density, the uniformity of the distribution is enhanced within each fragment (until some of them disappear, see, for example, curves (c) and (d) on Fig. 4) and the length of the regions with $i_1/i_{1\ell} = 1$, corresponding to the zones where the main reaction proceeds at the limiting diffusion current, increases.

Advantages of the three-layer electrode with variable conductivity of a matrix are evident from the dependence of the effective working thickness on the current density (Fig. 5). Though the shape of the dependence $L_{\mathrm{eff}} = f\,(i_{\mathrm{a}})$ is the same as for the one-layer electrode, the quantitative differences are substantial. The limiting value of L_{eff} increases from 0.28 to 0.78 cm, and the limiting current density, above which the current efficiency drops sharply, increases from 10 to 25 mA cm^{-2}. Thus, for the chosen parameters of polarization curve and electrodes, the use of the three-layer variant allows the working thickness of the PE to be increased almost three times with high values of the current efficiency of the main reaction being retained.

3.5. *Experimental investigation*

Experimental comparison of the performance of a three-layer electrodes made of materials having the same or different conductivity was carried out for the cathodic reduction of potassium ferricyanide on carbon fibres. Three carbon felts were chosen as the first approximation to an optimal three-layer set*. Physicochemical parameters of the materials are presented in Table 1.

Table 1. Characteristics of carbon felts used for the construction of the three-layer PE

*Type**	*Mass* /mg cm^{-2}	*Thickness* /cm	*Conductivity* /Ω^{-1}cm^{-1}
VNG-50-2	74.3	0.47	0.39
NTM-200	20.2	0.18	0.071
VVP-66-95	17.6	0.1	0.0021

*Materials designed and produced at the Institute of Electrocoal Materials, Electrougli, Moscow district, Russia.

Cylindrical tablets with a geometric surface area of 1 cm^2 were used. A PE with constant conductivity was built of three tablets of NTM-200, and the electrodes with variable conductivity were composed of tablets of different materials in the order indicated in Table 1 and also in the opposite order. Three-layer sets of the first and the second type were used as cathode in a flow-through cylindrical cell shown schematically in Fig. 6. The cathodic space was separated from the anodic space by a MK-40L cation-exchange membrane preventing the transfer of $\mathrm{Fe(CN)_6^{3-}}$ anions. The PE worked in the circulating regime with the use of electrolyte of the following composition: 0.01 M $\mathrm{K_3Fe(CN)_6}$+0.01 M $\mathrm{K_4Fe(CN)_6}$+1 M KOH. The linear solution rate was 1 cm s^{-1}, the solution volume 500 cm^3, and $t = 25\,^{\circ}\mathrm{C}$

The effective working surface of the PE was determined from the rate of $\mathrm{K_3Fe(CN)_6}$ concentration decrease in the delivery reservoir (d) with time. It is known that in a recirculation regime and with small conversion of the electroactive component for a single solution pass, the concentration–time behaviour is described by the following equation [16]:

$$\ln\frac{c_{\mathrm{t}}}{c_0} = -\frac{k_{\mathrm{m}}S_{\mathrm{eff}}}{V}t \tag{13}$$

This equation was obtained assuming that the working surface of the PE is not changed with time during electrolysis; for example, it works under the limiting current conditions from the beginning. If this is not true, the working surface can change because of the increase in the depth of main reaction penetration into the PE accompanied by the substantial decrease in the concentration of electroactive species in the circulating solution. To avoid these difficulties, the effective working surface of the PE, S_{eff}, under the given conditions was determined from Equation 13 in the initial stages of electrolysis and at the fixed (not high) recovery degree $R = 0.4-0.5$ using the known values of t and V.

Experimental values of the effective working surface (more precisely, the product $k_{\mathrm{m}} \times S_{\mathrm{eff}}$) for three variants of PE against the geometric current density are shown in Fig. 7. It is apparent that they are similar qualitatively to the theoretical ones (see Fig. 5), that is, with increasing current density the available surface for the main reaction increases in all cases up to a certain limit. Moreover, for the electrode with a favourable sequence of layers this limit is much higher, and for the unfavourable sequence it is lower than that for $\kappa_{\mathrm{s}} = \mathrm{const}$. The fact that the effective working surface is substantially (by a factor of

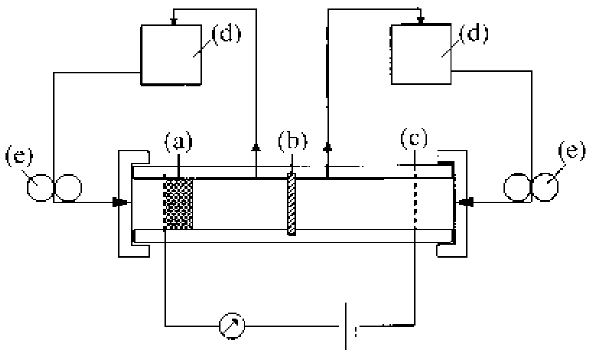

Fig. 6. Scheme of the experimental setup: (a) operating flow-through PE, (b) partition diaphragm, (c) counter electrode, (d) delivery reservoirs for catholyte and anolyte, (e) peristaltic pump.

---

* For the solution conductivity $\kappa_{\mathrm{L}} = 0.2\,\Omega^{-1}\,\mathrm{cm}^{-1}$ and total electrode thickness of 0.75 cm, an optimal set of κ_i (Ω^{-1} cm^{-1}) and L_i (cm) is the following: $\kappa_1 = 0.6$, $L_1 = 0.375$; $\kappa_2 = 0.099$, $L_2 = 0.255$; $\kappa_3 = 0.0174$, $L_3 = 0.12$.

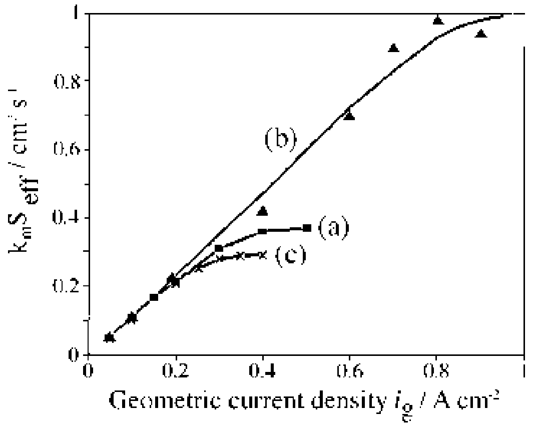

Fig. 7. Experimental dependence of effective working surface of PE (the product $k_m \times L_{eff}$) on geometric current density for the three types of three-layer electrode: composed of three layers of the same (a) and different (b), (c) carbon porous felts placed in the favourable sequence (as shown in Table 1) (b), and unfavourable sequence (opposite to that given in Table 1) (c). Continuous lines: 'best fit' curves passing through the points.

three) increased using the similar set of porous materials in their optimal sequence based on their conductivities is convincing evidence that the main effect is obtained due to the conductivity profile but not due to differences in other properties, for example differences in the kinetics of $K_3Fe(CN)_6$ reduction on different carbon materials. Together with this, the fact that the position of the curve (a) between the curves (b) and (c) is not symmetrical shows that the influence of layer sequence on the S_{eff} value is explained not only by the influence on the profile $\kappa_s(x)$.

Quantitative measurements of the current efficiency were not carried out, but it was noticed qualitatively that at the same geometric current density ($i_g > 0.4\,\mathrm{A\,cm^{-2}}$) hydrogen evolution on the 'composite' electrode built of different fibrous materials with a favourable sequence of layers was considerably weaker. Thus, the experiments confirm the possibility of significant increase in the PE working surface by using multilayer porous compositions with different conductivities with retention of high values of current efficiency of the main reaction.

Acknowledgements

The authors thank the Russian Foundation of Fundamental Research for financial support of this work (project 95-03-09661), Professor R.Yu. Beck for useful discussions, Mrs M. Kostirya and Mrs A. Panasenko for the assistance in numerical calculations and in carrying out the experiments.

References

[1] R. Yu. Beck, *Izvestiya SO AN SSSR*, ser. chim. nauk, vip. **6** (1977) 11.
[2] E. Mantzel, *Z. Electrochem.* **41** (1935) 10.
[3] L. I. Kadaner, *Zh. Phiz. Khim.* **59** (1955) 832.
[4] A. S. Hinman and G. Tang, *Electrochim. Acta* **36** (1991) 841.
[5] A. A. Vedenyapin, M. D. Baturova, S. V. Yushin and V. P. Timoshenko, *Galvanotekhnika i obrabotka poverkhnosti* **3** (1994) 45.
[6] M. Matlosz, *J. Electrochem. Soc.* **142** (1995) 1915.
[7] A. I. Masliy and N. P. Poddubny, *Elektrokhimiya* **14** (1978) 149.
[8] S. L. Tsapah and A. B. Umnov, *ibid.* **26** (1990) 914.
[9] A. I. Masliy and N. P. Poddubny *J. Appl. Electrochem.* **27** (1997) ■
[10] N. P. Poddubny and A. I. Masliy, *Sibirskii Khim. Zh.* vip. **3** (1991) 108.
[11] A. A. Konkin, 'Uglerodnie i drugie zharostoikie materiali', Moscow, "Khimiya" (1974) 376.
[12] V. K. Varentsov, A. F. Zherebilov and M. D. Malei *Izvestiya SO AN SSSR*, ser. chim. nauk, vip. **6** (1984) 120.
[13] A. F. Zherebilov and V. K. Varentsov. *ibid.*, vip. **1** (1987) 110.
[14] R. E. Sioda, *Electrochim. Acta* **16** (1971) 1569.
[15] R. Yu. Beck and A. P. Zamyatin, *Elektrokhimiya* **14** (1978) 1196.
[16] R. Yu. Beck, A.I. Masliy and T. A. Lavrova, *Izvestiya SO AN SSSR*, ser. chim. nauk, vip. **1** (1972) 25.